Electronic properties of the (100) (Si)/(Ge) strained-layer superlattices

Sashi Satpathy,* Richard M. Martin,† and Chris G. Van de Walle‡
Xerox Palo Alto Research Center, Palo Alto, California 94304
(Received 21 August 1987; revised manuscript received 20 June 1988)

By performing local-density pseudopotential calculations, we examine the electronic structure of the $(Si)_n/(Ge)_m$ $(n,m \sim 3-7)$ strained-layer superlattices and show how strain and the layer thicknesses interplay in determining the nature of the electron states. A group-theoretical discussion of the symmetry properties of the electron states as well as an analysis of the selection rules for dipole-allowed optical transitions are given. For the $(Si)_4/(s\text{-}Ge)_4$ (where s denotes strained) superlattice on which experiments have been reported, we find that the lowest-energy transition observed at 0.76 eV is *not* a direct transition. The lowest direct transition at ~ 1.1 eV is not optically allowed from symmetry considerations, with the lowest allowed direct transition occurring at ~ 1.2 eV. Strain in the superlattice layers is shown to have an important effect on the nature of electron states in the gap region. We show that thin superlattices grown on Ge or Si-Ge alloy substrates are promising candidates for direct band-gap materials.

I. INTRODUCTION

Semiconductor superlattices consisting of alternate layers of different materials provide extra dimensions for tailoring material properties. The combination of controlled variations in the composition, strain, and thickness of the layers provides electronic and optical properties unlike any ordinary bulk material.[1] Of particular note for the present work is the successful fabrication of (Si)/(Ge) strained-layer superlattices using molecular beam epitaxy, with each layer consisting of a few monolayers of the constituent material.[2] In such cases where the superlattice layers are ultrathin, they adopt the lattice dimensions of the underlying substrate in the plane of the layers and thus are strained with respect to their bulk lattice structures. Recently, measurements of the optical properties have been reported for a $(Si)_n/(Ge)_m$ superlattice with $n=m=4$ grown on a silicon substrate, with the important result that optical transitions occur at low energies which are unique to the superlattice.[3] The observation of these new transitions suggests the possibility that, in contrast to Si, Ge, or any of their alloys, (Si)/(Ge) superlattices may be direct band gap materials.

In this paper we examine theoretically the electronic structure of the strained layer $(Si)_n/(Ge)_m$ superlattices by performing band structure calculations using the density-functional pseudopotential method. Three types of strained superlattices are considered: (Si)/(s-Ge) (where s denotes strain), (s-Si)/(Ge), and (s-Si)/(s-Ge), which can be experimentally fabricated by growing the superlattice on Si, Ge, and $Si_{0.5}Ge_{0.5}$ substrates, respectively, and which illustrate the variations in the properties with strain. Optical experiments have been done on the first of these structures, grown using crystalline silicon as the substrate.[3] Our calculations are used to compare with the experimental results for this structure and to provide predictions about the band gaps for the other structures, which to our knowledge have not been studied experimentally. Further, we examine the electronic structure as a function of the layer thickness, $n,m \sim 3-7$. We find that the basic features of the electronic structure can be understood in terms of the strains, zone folding of the bands, and quantum confinement effects, and we examine the conditions under which the lowest energy gap in the superlattice is direct.

Since this work was completed several papers have appeared describing calculations on thin (Si)/(Ge) superlattices. At the end of the present paper we discuss the relationship of our work to that reported recently by others.

II. THEORETICAL METHODS

In the present work the electronic structure calculations are done within the local density approximation (LDA) to the density-functional theory,[4,5] using *ab initio* norm-conserving nonlocal pseudopotentials of Bachelet *et al.*[6] and a basis set of plane waves.[7] The present self-consistent calculations of the superlattice charge density and potential are similar to those done by Van de Walle and Martin[8] in their study of the band offset problem. In their work on (Si)/(Ge), the information for the band offsets was derived from the self-consistent charge densities and electronic potentials. Here we carry out the calculations to the same accuracy as in that work, using plane waves with energies up to 6 Ry and with 5–10 special points for calculation of the charge density; we refer the reader to Ref. 8 for an extensive analysis of the accuracy with respect to the cutoff on the plane waves, the special point sets used for the integrations over the Brillouin zone, and the iterations to self-consistency. In the present work, unlike Ref. 8, the results of the self-consistent calculations are used to predict the electronic structure of the superlattices themselves.

Since we examine the electronic structure of the superlattices in this paper, we must justify the accuracy with which we can predict the desired aspects of the electronic bands in the superlattice. It is well known that the LDA leads to large errors in the band gaps of semiconductors,[9] in particular, that the gap is essentially zero for Ge.[10] Nevertheless, to a rather good approximation the correct

experimental gaps are given by a rigid shift of the LDA gaps, in the case of both Si and Ge by about 0.6 eV.[8] In addition, it was shown in Ref. 8, based upon theoretical arguments as well as comparison to experiments,[11–15] that the LDA accurately describes both the changes in the bands due to strains[11–13] and the relative positions of the bands at interfaces of Si and Ge.[14,15] Thus we expect the bands in the superlattice to be given well by the LDA if we include the constant shift. There is, however, one additional point. We choose to do the calculations on the superlattices with a 6-Ry cutoff; this leads to bulk bands of both Ge and Si in the relevant band gap region which agree better with experiment. With this choice of cutoff the calculated gaps between the top of the valence band and the lowest conduction band near X are lower than the experimental values for both Si and Ge by 0.1 eV. These are the relevant states for the lowest energy transitions in the superlattice. The Ge Γ_2' state, however, has too high an energy by about 2.7 eV. Although this is a large error, this does not greatly affect the states which we consider here. This is because in the thin superlattices, the zone center state in Ge is strongly affected by quantum confinement effects and is shifted to high energies well away from the conduction band minima.

Therefore, we believe that our calculational method is adequate for obtaining electron states around the gap region for the systems with which we are concerned. Our choice of 6-Ry cutoff makes the computations much faster allowing us to study the electron states of a large number of (Si)/(Ge) superlattices with little or no loss of accuracy as far as electron states in the gap region are concerned. We will present the direct results of the calculations with a 6-Ry cutoff, with the provision that detailed comparison with experiment should be made with the gaps increased by 0.1 eV and additional shifts due to spin-orbit interactions included.

The strain conditions must be considered in our calculations. Depending on the substrate on which the superlattice is grown, one could have strain in one or the other material in the superlattice or a distribution of strain between the two materials. For a pseudomorphic interface, the lattice constant in the plane $a_\parallel$ remains the same throughout the structure, while the lattice spacing in the superlattice direction $a_\perp$ assumes a value different for each material. The values of $a_\parallel, a_\perp$ are determined from the condition of minimization of the macroscopic elastic strain energy. The lattice parameters for different strain situation were evaluated in Ref. 8. Based upon that work, the following values are used in our calculation. (a) (s-Ge)/(Si): $a_\parallel = 5.43$ Å $= a_\perp$(Si), $a_\perp$(Ge) $= 5.82$ Å; (b) (Ge)/ (s-Si): $a_\parallel = 5.65$ Å $= a_\perp$(Ge), $a_\perp$(Si) $= 5.26$ Å; (c) (s-Si)/ (s-Ge): $a_\parallel = 5.52$ Å, $a_\perp$(Si) $= 5.36$ Å, and $a_\perp$(Ge) $= 5.75$ Å.

III. GENERAL RESULTS FOR (Si)/(Ge) SUPERLATTICES

In this section we report results of our analysis of the electronic states in representative (Si)/(Ge) superlattices. In Secs. III A–III C we draw general conclusions on the nature of the states, which are illustrated by specific results for the case of $(Si)_4/(s\text{-}Ge)_4$. These results are further used in the discussion in Sec. V, where we compare the theoretical results with experiments on this particular superlattice. In addition, in Sec. IV we discuss the requirements of group theory on the states in the superlattices, which allow useful classifications and reveal some subtle effects of different layer thicknesses.

A. Superlattice bands and zone folding

The basic features of electron bands for the (Si)/(Ge) superlattice can be understood in terms of folded average bulk bands. This is true since bands of Si and Ge are very much alike, especially with the band offset of about 0.5 eV taken into account. [The values of band offset for average valence bands across (100) (Si)/(Ge) as calculated by Van de Walle and Martin[8] are $E^{\rm BO}_{(s\text{-Ge})/(\rm Si)} = 0.54$ eV, $E^{\rm BO}_{(s\text{-Ge})/(s\text{-Si})} = 0.53$ eV, and $E^{\rm BO}_{(\rm Ge)/(s\text{-Si})} = 0.51$ eV.] The differences in one-electron energies are generally much less than the characteristic width of the bulk bands $|E^{\rm Si}_{n,k} - E^{\rm Ge}_{n,k}| \ll W$, where W is the bandwidth of Si or Ge. This is especially true for the valence bands. Thus, with the exception of certain states discussed below, the bands of the superlattice are expected to be similar to the bulk bands, "folded" into the small Brillouin zone of the superlattice.

Figure 1 illustrates the similarity we find between folded Si bands and the Si-Ge superlattice bands. Such similarity also exists with the folded Ge bands but is not shown in the figure. Figure 1(a) shows bulk bands of Si folded according to the superlattice periodicity corresponding to the $(Si)_4/(s\text{-}Ge)_4$ superlattice. In the folded bands of bulk Si, out of the six valleys that form the conduction band bottom Δ^c, four (denoted by $\Delta^c_\parallel$) occur along k directions parallel to the layers, viz., Γ-$X_\parallel$, while 2 (denoted by $\Delta^c_\perp$) are folded onto Γ-Z, i.e., onto k directions perpendicular to the layers. In Fig. 1(a) the bands denoted by solid lines along Γ-$X_\parallel$ are the bands corresponding to the bulk Si lattice with two atoms in the unit cell. The dashed bands along Γ-$X_\parallel$ connect the new folded states at Γ to the $X_\parallel$ point and correspond to bulk bands along the lines from $(2\pi/a)(0,0,\frac{1}{2})$ to $(2\pi/a)(1,0,\frac{1}{2})$ and $(2\pi/a)(0,0,1)$ to $(2\pi/a)(1,0,1)$ in the bulk diamond Brillouin zone. This is because the k points $(2\pi/a)(0,0,\frac{1}{2})$ and $(2\pi/a)(0,0,1)$ in the diamond Brillouin zone are folded to the Γ point of the superlattice Brillouin zone. Figure 1(b) shows bands for the superlattice and they are seen to correspond to generally small perturbations on the folded bulk bands. Notice that for the superlattice of Fig. 1(b), where Ge is strained to match the Si lattice, the nonfolding $\Delta^c_\parallel$ forms the conduction band bottom, making it an indirect-gap material. Effects of strain on states in the gap region will be discussed later.

B. Confinement of superlattice states

A well-established major difference between the bulk bands of Si and Ge is that the Γ_2' state of Ge is below that in Si by about 3 eV. As a result, confinement in the superlattice increases the energy of the Γ_2' conduction state

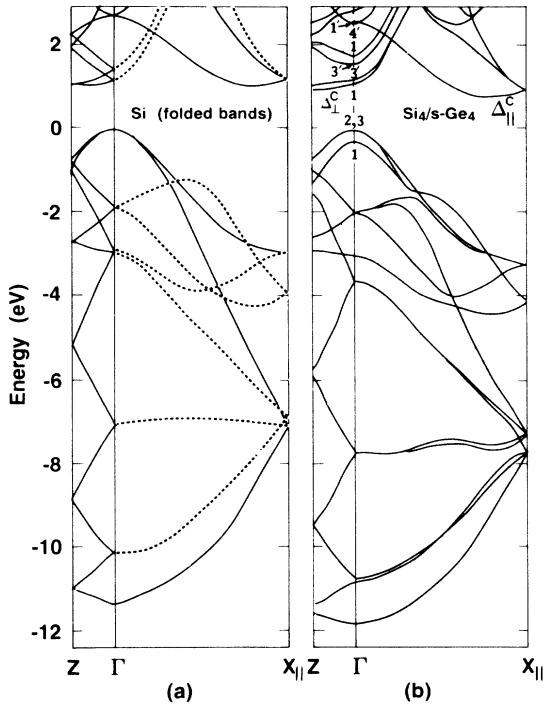

FIG. 1. Because of the remarkable overall similarity between valence as well as lower conduction bands in Si and Ge, the superlattice bands generally resemble folded bands of either Si or Ge. (b) shows the calculated bands for the $(Si)_4/(s\text{-}Ge)_4$ superlattice in which each superlattice layer consists of four Si or Ge monolayers. (a) shows the calculated bands for bulk Si folded according to the periodicity of the superlattice of (b). Bands denoted by solid lines between Γ-$X_{\parallel}$ in (a) indicate the unfolded bands of Si in the diamond Brillouin zone. Here $Z=(\pi/T_z)(0,0,1)$ with T_Z being the z component of the translational periodicity in the superlattice direction. $X_{\parallel}=(2\pi/a_{\parallel})(1,0,0)$ referred to the cube directions in the diamond structure.

which is mostly confined to Ge. Taking a value of $m^*=0.04m_e$ and a barrier height of ~ 3 eV, we estimate from a Kronig-Penney–type model that because of the confinement, Ge-$\Gamma_2'^c$ moves up in energy by 2.1–2.7 eV for Ge layer thickness of 3–6 monolayers. The conduction band bottom at the L point experiences a similar effect, but reduced in magnitude. The entire conduction band joining Γ_{15} to X_1 in Si or Ge, on the other hand, does not experience as much confinement effect because of small barrier heights. Thus the lowest conduction bands are made up primarily of these states. As discussed above our pseudopotential calculation reproduces reasonably the experimental energies of the entire conduction band along Δ^c joining Γ_{15}-X_1, with the calculated values of the Δ^c states around the conduction band minimum about 0.1 eV below experiment for both Si and Ge. Thus, in spite of the fact that in our calculation $\Gamma_2'^c$ is not reproduced well for Ge, we expect that the electron states around the band gap in the superlattices should be described well.

C. Wave functions

In Fig. 2 we show the charge density corresponding to the wave functions for the superlattice bands shown in Fig. 1(b): the top three valence bands and the lowest six conduction bands at the Γ point, as well as the lowest

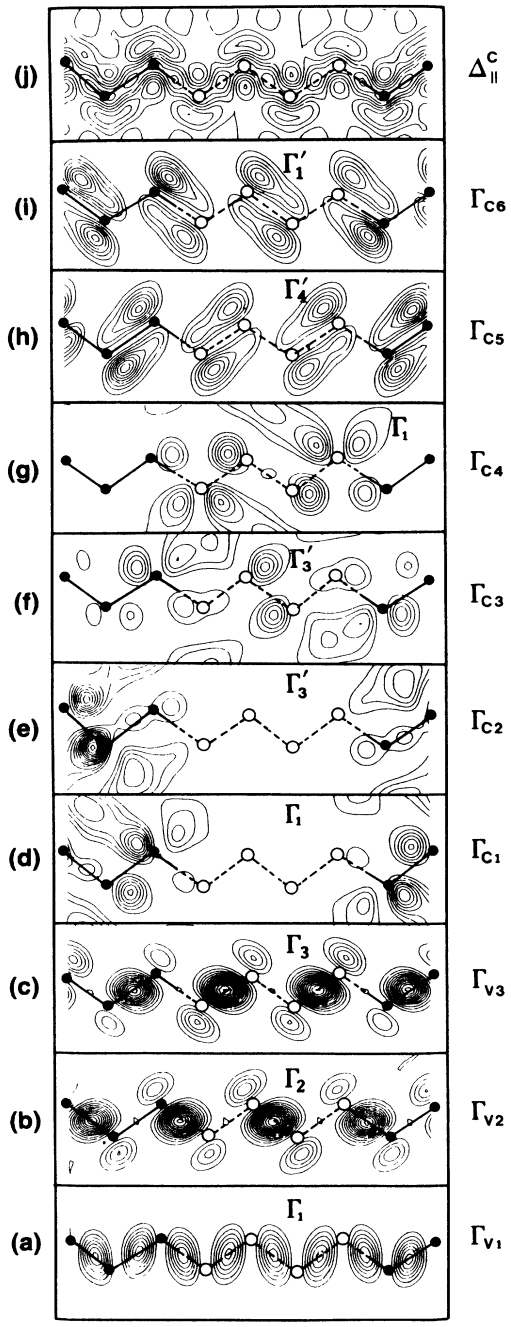

FIG. 2. Contour plots of pseudo-charge-densities of individual states in the $(Si)_4/(s\text{-}Ge)_4$ superlattice on a plane containing (Si)/(Ge) chains. Open circles denote Ge atoms and solid circles denote Si atoms. The highest three valence states (a), (b), and (c) are spread out in both Si and Ge layers almost uniformly. The lowest two conduction states (d) and (e) are confined to Si, while the next two higher states, (f) and (g), are confined to Ge. The $\Delta_{\parallel}^c$ state (j) forms the bottom of the conduction bands.

conduction band, labeled $\Delta_{\parallel}^{c}$ which has a large wave vector parallel to the planes. It is immediately clear that some states are very delocalized in both Si and Ge, whereas others are quite confined. These effects can be understood as follows. The top of the valence bands are delocalized because their masses correspond to a valence bandwidth much larger than the confinement barrier of about 0.5 eV resulting from the differences between Si and Ge. The confinement is even less for the state at $\Delta_{\parallel}^{c}$. In this case the appropriate mass for motion in the direction perpendicular to the layers is the transverse effective mass for the Δ minimum in the bulk, which is only $0.2m_e$. The confinement barrier is extremely small (0.1 eV) as shown by the theoretical results of Ref. 8 and by experimental measurements on thick layers.[14,15] The situation is different, however, for the lowest four conduction bands of the superlattice at Γ. These are formed from bands folded from the Δ point: the appropriate mass is the heavy longitudinal mass, about $1.0m_e$, and the confinement barrier is much larger, around 0.7 eV (see Figs. 5 and 7 of Ref. 8). Thus the lowest two conduction states at Γ are confined mainly to the Si layers. The next two higher ones are localized in Ge. The analysis of Ref. 8 shows that these general conclusions apply to other thicknesses of the layers and to other strain conditions as well.

D. Effects of strain

Strain in the superlattice plays an important role in determining whether the gap is direct or indirect. In the folded bands of bulk Si, out of the six valleys that form the conduction band bottom Δ^{c}, four occur essentially unchanged along Γ-$X_{\parallel}$ (denoted by $\Delta_{\parallel}^{c}$) while two are folded onto Γ-Z (denoted by $\Delta_{\perp}^{c}$). Strain splits the $\Delta_{\parallel}^{c}$ and $\Delta_{\perp}^{c}$ states, increasing the energy of one type while lowering that of the other. The magnitude of the strain splitting is large enough to govern the resulting properties of the superlattice. In Fig. 3 we show the resulting bands of the 4-4 superlattice for three different strain conditions. We see that in the case of $(Si)_4/(s\text{-}Ge)_4$ superlattice, $\Delta_{\perp}^{c}$ is well above $\Delta_{\parallel}^{c}$, whereas for $(s\text{-}Si)_4/(Ge)_4$, $\Delta_{\perp}^{c}$ is the lowest conduction band state, leading to the possibility of a direct gap. The cases of $(s\text{-}Si)_4/(s\text{-}Ge)_4$ is intermediate, with the two states having about the same energy within the accuracy of our calculations. These results concerning effects of strain remain unchanged when the layer thickness is varied.

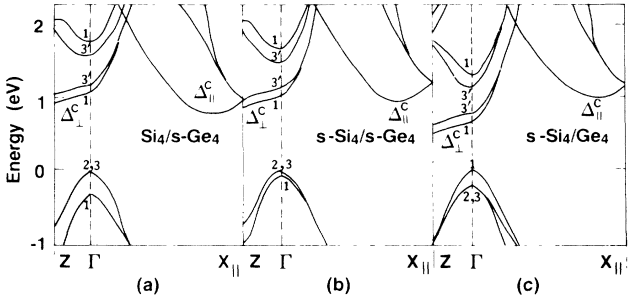

FIG. 3. Calculated electron bands in the gap region for the (Si)/(Ge) superlattice with different strain conditions: (a) $(Si)_4/(s\text{-}Ge)_4$, (b) $(s\text{-}Si)_4/(s\text{-}Ge)_4$, and (c) $(s\text{-}Si)_4/(Ge)_4$. $\Delta_{\parallel}^{c}$ ($\Delta_{\perp}^{c}$) refers to the nonfolding (folding) conduction band bottom state in Si in the diamond structure. In case (a), the nonfolding $\Delta_{\parallel}^{c}$ state is below the folding $\Delta_{\perp}^{c}$ state; consequently, for this strain type there is no possibility of a direct gap. In case (c), strain raises energy of the $\Delta_{\parallel}^{c}$ state above that of the $\Delta_{\perp}^{c}$ state with the possibility of a direct gap for this strain type. For case (b) these states occur close in energy.

Strain also affects the uppermost states in the valence band. Although the valence-band maximum always occurs at the Γ point, a result expected from folding of the bulk bands, the order of the valence bands at Γ nevertheless changes. The uniaxial strain splits the original threefold degenerate valence top into (almost) doubly degenerate p_x-p_y states and a nondegenerate p_z state. The order of these two states and the magnitude of the splitting depends on the type of strain as seen from Fig. 3.

Our pseudopotential calculations do not include the effect of spin-orbit coupling which is not negligible especially for Ge. The S-O splitting of the valence-band top at the Γ point for Ge, $\Delta_0 \approx 0.30$ eV. The wave function of the superlattice valence top is, to a very good approximation, equally spread out in both Si and Ge layers of the superlattice, as has already been seen from Fig. 2. With this assumption, and following the analysis of Pollak and Cardona[11] we get the following shift in the valence top with respect to the weighted average:

$$E_{v_1} = -\frac{\Delta_0}{6} + \frac{\delta E_{001}}{4} + \tfrac{1}{2}(\Delta_0^2 + \Delta_0 \delta E_{001} + \tfrac{9}{4}\delta E_{001}^2)^{1/2} , \tag{1a}$$

$$E_{v_3} = -\frac{\Delta_0}{6} + \frac{\delta E_{001}}{4} - \tfrac{1}{2}(\Delta_0^2 + \Delta_0 \delta E_{001} + \tfrac{9}{4}\delta E_{001}^2)^{1/2} , \tag{1b}$$

$$E_{v_2} = \frac{\Delta_0}{3} - \frac{\delta E_{001}}{2} . \tag{1c}$$

Here, Δ_0 is the magnitude of the splitting of the Γ_{15} valence-band top due to spin-orbit coupling,

$$\Delta_0 = \frac{n_{\mathrm{Ge}}}{n_{\mathrm{Ge}} + n_{\mathrm{Si}}} \Delta_0^{\mathrm{Ge}} + \frac{n_{\mathrm{Si}}}{n_{\mathrm{Ge}} + n_{\mathrm{Si}}} \Delta_0^{\mathrm{Si}} , \tag{2}$$

where n_{Ge} (n_{Si}) is the number of monolayers in each Ge (Si) layer of the superlattice, $\Delta_0^{\mathrm{Ge}} \simeq 0.30$ eV and $\Delta_0^{\mathrm{Si}} \simeq 0.04$ eV. From Eq. (1) the magnitude of splitting due to strain only is $\frac{3}{2}\delta E_{001}$; this is the quantity by which the valence top splits in our calculations. This value can also be estimated from the measured deformation potentials;

$$\delta E_{001} = \left[2b_{\mathrm{Ge}} \frac{a_{\perp}^{\mathrm{Ge}} - a_{\parallel}^{\mathrm{Ge}}}{a_{\mathrm{Ge}}} \right] \frac{n_{\mathrm{Ge}}}{n_{\mathrm{Ge}} + n_{\mathrm{Si}}} + \left[2b_{\mathrm{Si}} \frac{a_{\perp}^{\mathrm{Si}} - a_{\parallel}^{\mathrm{Si}}}{a_{\mathrm{Si}}} \right] \frac{n_{\mathrm{Si}}}{n_{\mathrm{Ge}} + n_{\mathrm{Si}}} , \tag{3}$$

with $b_{\mathrm{Ge}} = -2.86 \pm 0.15$ eV (Ref. 12) and $b_{\mathrm{Si}} = -2.1 \pm 0.1$ eV (Ref. 13). We find that the valence-top splitting in our

calculation agrees extremely well with the value obtained from Eq. (3). Some results will be given later in Fig. 7(b).

IV. CONSEQUENCES OF SYMMETRY AND DIPOLE SELECTION RULES

The superlattices $(Si)_n/(Ge)_m$ can be classified by their symmetries, which have interesting changes for different layer thicknesses n and m. In particular, if either n or m is even, there is a center of inversion at the center of an even layer. Either n or m must be odd for the existence of a fourfold axis perpendicular to the layers. The latter may be seen by noting that if n and m are both even, the Si-Ge bonds are all oriented parallel to one plane, viz., the x-z plane, where z is the [001] direction perpendicular to the layers and x is one of the [110] directions in the usual cubic notation. Depending on whether n and m are even or odd, there are three distinct cases as follows.

(1) *Both n and m even.* If the origin is placed on an atom in one of the two innermost monolayers of either layer, the symmetry operations of the factor group of the translation group are E, σ_x, σ_y, $\sigma_z(f_1)$, $I(f_1)$, $C_{2x}(f_1)$, $C_{2y}(f_1)$, and C_{2z}. Our coordinate system here is such that z is along the superlattice direction and the x and y axes are rotated by 45° with respect to the conventional cube axes in the diamond structure. The nonsymmorphic operations involve a fractional translation $f_1=(a_\parallel/4, a_\parallel/4, a_\perp/4)$ referred to the cube axes, where $a_\parallel$ and $a_\perp$ denote the lattice constants of the chosen layer, which is, in general, strained so that $a_\parallel \neq a_\perp$. The point symmetry is D_{2h}, which has eight single representations (all singly degenerate) and only two double representations (both doubly degenerate). Throughout this paper we shall follow the standard Bouckaert-Smolukowski-Wigner-Elliot (BSWE) notations[16] for the single and double representations. The double representations of the D_{2h} group will be denoted simply by Γ^+ and Γ^-; the former is inversion symmetric and the latter is antisymmetric.

(2) *Both n and m odd.* We consider the origin to be placed on an atom in the central monolayer of either of the two odd layers. For this superlattice there is no center of inversion, but inversion coupled with a fourfold rotation is a symmetry operation. The point symmetry in this case if D_{2d} with the following symmetry elements: E, σ_x, σ_y, C_{2z}, IC_{4z}, IC_{4z}^{-1}, C_{2xy}, and $C_{2x\bar{y}}$. The D_{2d} point group has in total five single representations (only of these being doubly degenerate and the rest nondegenerate) and only two double representations (both doubly degenerate).

(3) *n odd and m even, or vice versa.* Unlike the previous two cases, the translational periodicity in the z direction is doubled, i.e., the unit cell of the superlattice now contains *two* Si and *two* Ge layers. The two layers are not translationally equivalent since one even layer is rotated by 90° with respect to the other. With the origin placed on an atom in an innermost monolayer of the even-layered material, the factor group of the translation group now contains 16 elements: E, σ_x, σ_y, $\sigma_z(f_1)$, $I(f_1)$, $C_{2x}(f_1)$, $C_{2y}(f_1)$, C_{2z}, $C_{4z}(f_2)$, $C_{4z}^{-1}(f_2)$, $C_{2xy}(f_1+f_2)$, $C_{2\bar{x}y}(f_1+f_2)$, $\sigma_{\bar{x}y}(f_2)$, $\sigma_{xy}(f_2)$, $IC_{4z}(f_1+f_2)$, and $IC_{4z}^{-1}(f_1+f_2)$. Here, as before, $f_1=(a_\parallel/4, a_\parallel/4, a_\perp/4)$ in the cube coordinates and f_2 is a partial translation connecting two inequivalent layers of the same material. The point symmetry in this case is D_{4h}.

The correspondence between single and double representations for the D_{2h}, D_{2d}, and D_{4h} groups are trivially obtained; however, for ready reference they are given in Table I. The dipole-allowed transitions are listed in Table II. These dipole selection rules are relevant for optical transitions at the Γ point of the superlattice. Although we do not predict quantitatively large effects from the changes in symmetry, these are novel, potentially useful, properties of the superlattice. Below we examine the case of $(Si)_4/(s\text{-}Ge)_4$ in some detail.

V. OPTICAL TRANSITIONS FOR $(Si)_4/(Ge)_4$ SUPERLATTICES

A. $(Si)_4/(s\text{-}Ge)_4$ lattice matched to Si

For the $(Si)_4/(s\text{-}Ge)_4$ superlattice, the chains formed by the Si-Ge bonds at every interface run along the same direction, which by convention is the direction of our x axis. The y axis is perpendicular to x in the plane of the interface, and the z axis is along the superlattice direction. The point-group symmetry of the $(Si)_4/(s\text{-}Ge)_4$ superlattice is the orthorhombic D_{2h} group as discussed above. The space group, like in the case of diamond, is nonsymmorphic as some elements of the space group involve fractional lattice translations. At the Γ point, the small point group of k is of course the entire group D_{2h}.

The symmetries of electron states at the Γ point of the superlattice and the dipole-allowed transitions are shown in Fig. 4. All states are nondegenerate apart from spin degeneracy. The triply degenerate Γ_{25}' state forming the valence top in bulk crystals splits up into three nondegenerate states in the superlattice into a $\Gamma_1+\Gamma_2+\Gamma_3$ symmetry combination of the D_{2h} group. Of these, Γ_2 and Γ_3 are almost degenerate and are split from the lowest Γ_1 by about 0.3 eV. As we mentioned earlier, our calculations do not reproduce well the Γ_2' conduction state in Si or Ge in the diamond structures. In the superlattice, we estimate that because of the confinement effect, the corre-

TABLE I. Correspondence between single and double representations for D_{2h}, D_{2d}, and D_{4h} point groups.

D_{2h}	Γ_i	Γ_1	Γ_2	Γ_3	Γ_4	
		Γ_1'	Γ_2'	Γ_3'	Γ_4'	
	$\Gamma_i\times D_{1/2}$	Γ^+	Γ^+	Γ^+	Γ^+	
		Γ^-	Γ^-	Γ^-	Γ^-	
D_{2d}	Γ_i	Γ_1	Γ_1'	Γ_2	Γ_2'	Γ_3
	$\Gamma_i\times D_{1/2}$	Γ_6	Γ_7	Γ_6	Γ_7	$\Gamma_6+\Gamma_7$
D_{4h}	Γ_i	Γ_1	Γ_2	Γ_3	Γ_4	Γ_5
		Γ_1'	Γ_2'	Γ_3'	Γ_4'	Γ_5'
	$\Gamma_i\times D_{1/2}$	Γ_6^+	Γ_7^+	Γ_7^+	Γ_6^+	$\Gamma_6^+ + \Gamma_7^+$
		Γ_6^-	Γ_7^-	Γ_7^-	Γ_6^-	$\Gamma_6^- + \Gamma_7^-$

TABLE II. Dipole-allowed transitions for the (100) $(Si)_n/(Ge)_m$ superlattices at the Γ point. The symmetry classifications and the dipole selection rules are independent of the strain condition, i.e., they are valid whether the Si, Ge, or both layers are strained corresponding to growth on different substrates. They depend only on the thicknesses n and m of the Si and Ge layers.

$(Si)_n/(Ge)_m$	Point group	Polarization[a]	Allowed transitions	
			Single Reps.	Double Reps.
n,m even	D_{2h}	x,y	$\Gamma_1,\Gamma_4\leftrightarrow\Gamma_1',\Gamma_4'$; $\Gamma_2,\Gamma_3\leftrightarrow\Gamma_2',\Gamma_3'$	$\Gamma^+\leftrightarrow\Gamma^-$
		z	$\Gamma_1\leftrightarrow\Gamma_3'$; $\Gamma_2\leftrightarrow\Gamma_4'$; $\Gamma_3\leftrightarrow\Gamma_1'$; $\Gamma_4\leftrightarrow\Gamma_2'$	$\Gamma^+\leftrightarrow\Gamma^-$
n,m odd	D_{2d}	x,y	$\Gamma_1,\Gamma_1',\Gamma_2,\Gamma_2'\leftrightarrow\Gamma_3$	all allowed
		z	$\Gamma_2\leftrightarrow\Gamma_1',\Gamma_1\leftrightarrow\Gamma_2'$	$\Gamma_6\leftrightarrow\Gamma_7$
One odd, other even	D_{4h}	x,y	$\Gamma_1,\Gamma_2,\Gamma_3,\Gamma_4\leftrightarrow\Gamma_5'$; $\Gamma_1',\Gamma_2',\Gamma_3',\Gamma_4'\leftrightarrow\Gamma_5$	$\Gamma_6^+,\Gamma_7^+\leftrightarrow\Gamma_6^-,\Gamma_7^-$
		z	$\Gamma_1\leftrightarrow\Gamma_4'$; $\Gamma_2\leftrightarrow\Gamma_3'$; $\Gamma_3\leftrightarrow\Gamma_2'$; $\Gamma_4\leftrightarrow\Gamma_1'$; $\Gamma_5\leftrightarrow\Gamma_5'$	$\Gamma_6^+\leftrightarrow\Gamma_6^-$; $\Gamma_7^+\leftrightarrow\Gamma_7^-$

[a]The x,y (z) transitions are allowed if light is incident perpendicular (parallel) to the superlattice planes.

sponding state would occur about 2.7 eV above the valence top, i.e., around the Γ_1' and Γ_4' states.

For dipole-allowed optical transitions, the matrix element $\langle\Psi_i|\mathbf{r}|\Psi_f\rangle$ is nonzero, where $\mathbf{r}$ is along the direction of the polarization of light. If light is incident perpendicular to the superlattice planes, $\mathbf{r}$ lies in the plane of the interface, and the x or y transitions are allowed. As seen from Fig. 4, transition to the lowest conduction state at the Γ point is not dipole allowed. Because the superlattice bands are in general only slightly perturbed from the folded bulk bands, as illustrated in Fig. 1, the matrix elements for the new optical transitions with no counterpart in the bulk are expected to be small, even though these optical transitions are dipole allowed.

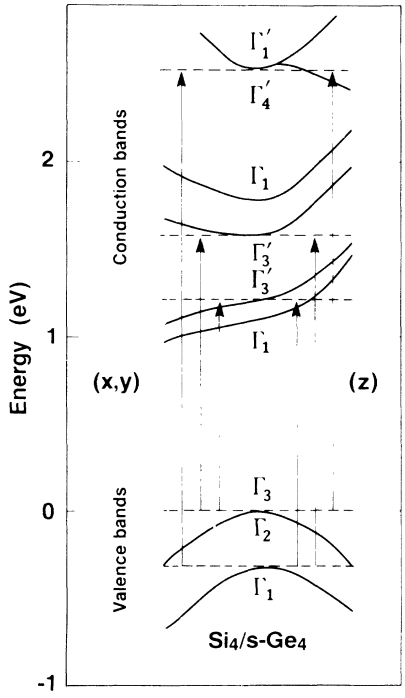

FIG. 4. Energy bands near the Γ point for the $(Si)_4/(s\text{-}Ge)_4$ superlattice and dipole-allowed optical transitions for plane-polarized light. Transitions from the valence states at Γ shown in the figure to the lowest conduction state of Γ_1 symmetry are forbidden. The x,y (z) transitions are allowed for light incident perpendicular (parallel) to the superlattice planes.

Our calculation does not take into account the spin-orbit (SO) coupling. When this is included, we estimate that the difference in energy between Γ_2 and Γ_3 would be about 0.1 eV. Furthermore, inclusion of the SO coupling allows some of the forbidden transitions by admixing various states. In fact, in the present case all inversion-symmetric states mix among one another as also do the inversion-antisymmetric states. This can be seen in Table I from the fact that there are only two double representations of the D_{2h} group, denoted by Γ^+ and Γ^-, respectively. In Fig. 4 all unprimed states are symmetric and transform according to the Γ^+ representation when SO coupling is taken into account, while the primed states are antisymmetric transforming according to Γ^-. Thus optical transitions from all unprimed states to primed states and vice versa are allowed. However, in the present case, the strength of the allowed transitions which were forbidden but for the SO coupling would be small from consideration of energetics of various orbitals.

From our calculation, the energy of the lowest direct transition is about 1.1 eV; however, this transition is not dipole allowed. The lowest dipole-allowed direct transition occurs at 1.2 eV, which is dipole allowed for light with x,y polarization. In the optical measurements on this superlattice reported in Ref. 3, there are transitions around 1.25 eV which we identify with this direct transition. Our calculations indicate an indirect gap at 0.8 eV, as shown in Fig. 1. As mentioned above, our calculations underestimate the values for Δ^c in the bulk crystals by about 0.1 eV for both Si and Ge. We expect the calculated transition energies for the lowest gaps in the superlattice to also be low by this amount. On the other hand, inclusion of SO coupling would reduce the lowest transition energy by about 0.05 eV. In addition, there may be exciton effects which lower the transition energy; however, we anticipate this effect to be small since the experimental exciton binding energies in the bulk are only ~ 15 meV in Si and ~ 5 meV in Ge.[17] Taking all these factors into account, we believe our result for the lowest transition to be accurate to within about 0.1 eV. Therefore we believe our results indicate that the experimentally observed lowest transition of 0.76 eV is not a direct transi-

tion. Instead, this observed energy agrees very well with our value for the indirect gap of 0.8 eV mentioned above. A possible explanation is that the experimental observation may be an indirect transition which has large strength due to imperfection of the interface or some other extrinsic effect in the superlattice.

B. $(s\text{-Si})_4/(\text{Ge})_4$ and $(s\text{-Si})_4/(s\text{-Ge})_4$ lattice matched to Ge and $\text{Si}_{0.5}\text{Ge}_{0.5}$

The primary effect of the strain conditions (by matching to substrates with larger lattice constants, such as Ge or Si-Ge alloys) is to increase the energy of the indirect $\Delta_{\parallel}^{c}$ gap and lower the potentially direct gap of the folded $\Delta_{\perp}^{c}$ states. The analysis of dipole-allowed transition for $(s\text{-Si})_4/(\text{Ge})_4$ or $(s\text{-Si})_4/(s\text{-Ge})_4$ is similar to the case of $(\text{Si})_4/(s\text{-Ge})_4$ just discussed. This can be done by inspecting the symmetries of bands given in Fig. 3 and the dipole selection rules given in Table II. As in the case of $(\text{Si})_4/(s\text{-Ge})_4$, for all three strain types, optical transitions from the highest three valence states to the lowest conduction state of Γ_1 symmetry are dipole forbidden. The case of $(s\text{-Si})_4/(\text{Ge})_4$ is different from the other two in that here the lowest allowed direct transition involves light with z polarization, as may be seen by inspecting Figs. 3 and 4. Analysis of polarization dependence of optical transition experimentally could shed light on the nature of the lowest transition experimentally observed.

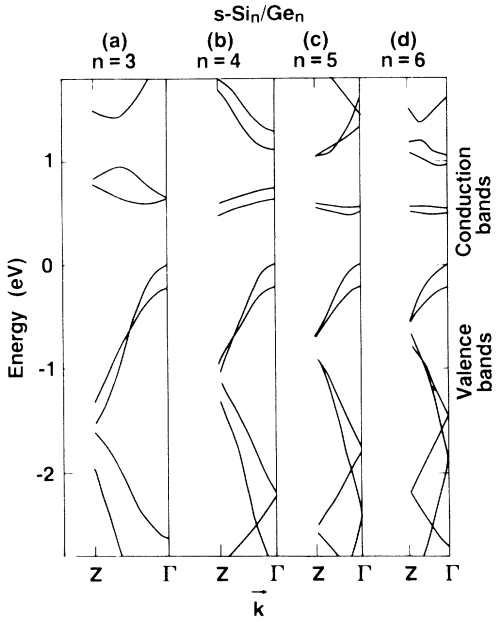

FIG. 5. Energy bands along the Γ-Z direction for the $(s\text{-Si})_n/(\text{Ge})_n$ ($n=3$, 4, 5, or 6) superlattice. As discussed in the text for this strain condition, $\Delta_{\parallel}^{c}$ is above $\Delta_{\perp}^{c}$ and the superlattice is potentially a direct gap material. For the case $n=3$ or 4, the gap is clearly indirect [(a) and (b)], while for $n=5$ or 6 the calculated gap is barely indirect; however, in the latter two cases our calculations are not accurate enough to rule out direct gaps.

VI. VARIATION OF THE BANDS WITH LAYER THICKNESSES

The superlattice bands can be altered by changing the layer thickness of the Si layer or of the Ge layer or by changing both thicknesses. We first consider the case of $(s\text{-Si})_n/(\text{Ge})_n$ superlattices where the Si and Ge superlattice layers have the same number of monolayers. Because Si is strained, the nonfolding $\Delta_{\parallel}^{c}$ occurs above the folding $\Delta_{\perp}^{c}$ (Fig. 3) so that a direct gap is a possibility. We have still to examine whether the conduction band bottom would occur at the zone center or only near it by performing actual calculations. In the folded bands, the Γ point is always folded to the zone center of the superlattice Brillouin zone. The X point, on the other hand, is folded to Γ or Z, depending on whether n is even or odd. Therefore in the simple zone-folding scheme, the valence top for the superlattice always occurs at the Γ point, while the conduction band bottom $\Delta_{\min}^{c}$ is folded to different k points depending on the layer thickness. From Fig. 5 we find that for $n=3$ or 4 the gap is indirect, with the conduction band minimum occurring along the Γ-Z direction. For $n=5,6$ we find a near-direct gap. However, the energy difference between the direct gap and the indirect gap for $n=5,6$ as seen from Fig. 5 is very small, and within the accuracy of our calculations we cannot say if the gaps in these two cases should be direct or indirect. Potentially they are candidates for direct-gap materials.

Another way of modifying the superlattice bands which we examine here would be to keep the superlattice periodicity unchanged while varying the thicknesses of the two individual layers. In particular, we examine the case of $(s\text{-Si})_n/(\text{Ge})_m$ where both n and m are varied in such a way that $n+m=10$. The folded bands are essentially unchanged by this variation; therefore the superlattice bands displayed in Fig. 6 greatly resemble one another. As the thickness of the Si layer decreases, the conduction bands shift up and so do gap values as seen from Figs. 6 and 7(a). On the other hand, the energy of the nonfolding $\Delta_{\parallel}^{c}$ with respect to the valence top remains more or less unaffected as illustrated in Fig. 7(a). Qualitatively, this is apparent from the fact that the wave function corresponding to the $\Delta_{\parallel}^{c}$ is well spread out in both Si and Ge layers. We see from Fig. 7(a) that the gap can be varied significantly by changing the layer thicknesses.

In Fig. 7(b) the splitting of the valence-band top as obtained from Eqs. (1)–(3) (dashed line) as well as the calculated values are shown. Agreement between these two is consistent with the fact that valence states are about equally spread out in Si and Ge. Our calculations as mentioned earlier does not include spin-orbit coupling. When this is included the splitting of the valence top as obtained from Eqs. (1)–(3) for the case $n+m=10$ is indicated by solid lines in Fig. 7(b). This is the full splitting of the valence top in the real superlattice.

VII. SUMMARY

In summary, we have examined the electronic properties of strained-layer (100) $(\text{Si})_n/(\text{Ge})_m$ superlattices by performing local-density pseudopotential calculations. The lowest conduction band states are found to originate from the six Δ^{c} minima in bulk Si and Ge. In the super-

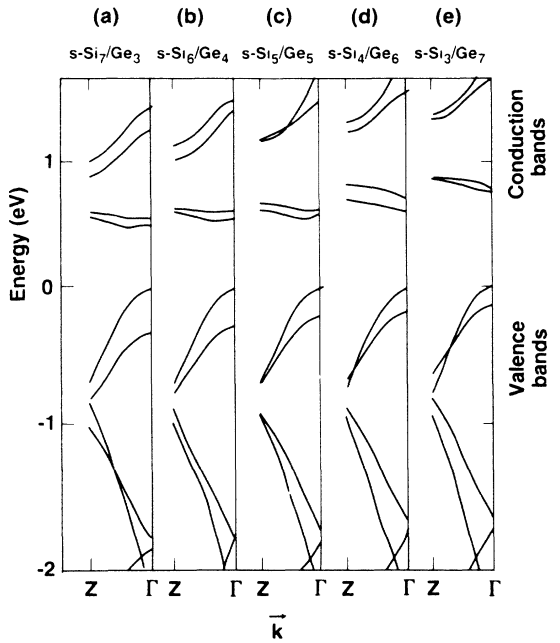

FIG. 6. Energy bands along Γ-Z for some $(s\text{-Si})_n/(\text{Ge})_m$ superlattices with $n+m=10$. This strain condition affords the possibility of a direct-gap material by placing $\Delta_{\parallel}^{c}$ above $\Delta_{\perp}^{c}$ in energy. Indeed we see that from our calculations, two of these have direct gaps, (d) and (e), while the rest have near-direct gaps. Notice the close similarity between the bands for the different superlattices shown here. This is because the effect of zone folding is essentially the same with $n+m$ fixed.

lattice these split into four $\Delta_{\parallel}^{c}$ states which give indirect gaps, and two $\Delta_{\perp}^{c}$ states, which are folded to near $k=0$ by the superlattice periodicity. The latter lead to direct or nearly direct gaps. Strain was shown to be the dominant factor which controls the relative energies of these states, modifying the conduction bands in such a way that the indirect $\Delta_{\parallel}^{c}$ states are lower for the (Si)/(s-Ge) superlattice which is lattice matched to a Si substrate. We conclude that, in recent experiments on $(\text{Si})_4/(s\text{-Ge})_4$, the lowest energy transition observed at 0.76 eV is not a direct transition. On the other hand, we find that the states derived from $\Delta_{\perp}^{c}$ are lower for (s-Si)/(Ge) matched to Ge or (s-Si)/(s-Ge) matched to $\text{Ge}_{0.5}\text{Si}_{0.5}$, allowing the possibility of direct band gaps in these superlattices. Our calculations indicate that in these cases, the $(s\text{-Si})_n/(\text{Ge})_n$ superlattice may have direct gaps for $n=5$ or 6, whereas for $n=3$ or 4 the minimum in the conduction band occurs away from the Γ point. In addition, we found that the band gaps in the $(\text{Si})_n/(\text{Ge})_m$ superlattice may be tuned by varying n and m while keeping $n+m$ fixed. Our calculations indicate that $(s\text{-Si})_4/(\text{Ge})_6$ and $(s\text{-Si})_3/(\text{Ge})_7$ superlattices should be direct-gap materials. Selection rules for the dipole-allowed transitions were obtained for the general $(\text{Si})_n/(\text{Ge})_m$ superlattice. The theoretical discussions presented here should provide motivations for future experiments on the electronic states and optical properties of the (Si)/(Ge) superlattices.

Since this work was completed, several papers have appeared describing related calculations on (Si)/(Ge) superlattices.[18–23] The major conclusions of the energies of the direct transitions in the superlattices agree with the present work. Density-functional (LDA) calculations very similar to those presented here are reported in two papers.[21,22] The primary difference is that in these papers the bands are calculated with large cutoffs on the plane

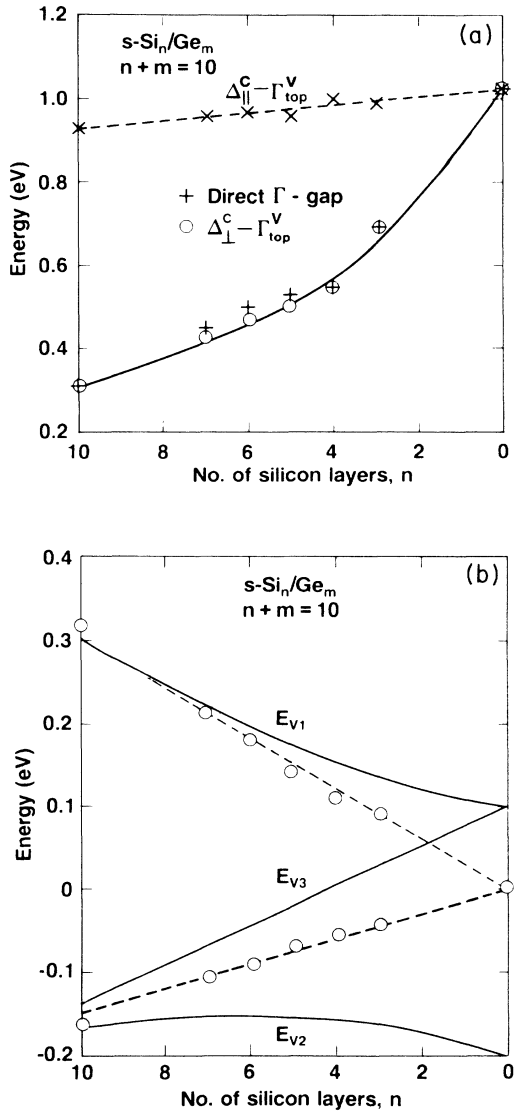

FIG. 7. (a) Variation of gap values as a function of thickness of Si layers. Notice that the end members are simply Ge or strained Si and the values shown for these correspond to the bulk bands folded to the superlattice Brillouin zone. The fact that $\Delta_{\parallel}^{c}$ is above $\Delta_{\perp}^{c}$ in Si is caused by the uniaxial strain, as discussed in the text. The "corrected" gap values are to be obtained by shifting up the values shown in the figure by about 0.1 eV except for small values of n ($n \approx 2$ or less). In the latter case, additional states associated with Ge-L_1 and Ge-Γ_2' would have energies lower than the Ge-Δ^c. (b) The valence-top splitting obtained from our calculation (circles) is compared with Eqs. (1)–(3) (dashed lines). Both of these omit SO coupling. The solid line shows the estimated valence-band splitting when both the SO coupling and strain are taken into account for the case $n+m=10$. For a general case of n and m and strain condition, the splitting may be obtained from Eqs. (1)–(3).

waves (12–15 Ry). By applying the shift of 0.6 eV to their results, the energies are in very good agreement with our results shifted by 0.1 eV, exactly as anticipated in our discussion in Sec. II. The symmetries of the lowest energy states appear to agree with our assignments given in Fig. 4. References 21 and 22 have also calculated optical transition matrix elements (which we have not done) with the conclusion that the new superlattice transitions have very small strength. The present work has gone further than the others in analysis of the symmetries and quantitative calculations for layers with various thicknesses, in particular, ones containing odd numbers of atomic layers, which are not considered at all in any other paper to our knowledge. As discussed in the summary and shown in Figs. 5 and 6, we find such variations in layer thicknesses are particularly promising for creation of direct gap superlattices.

Hybertsen and Schluter[22] have also carried out full quasiparticle calculations for electronic energies in the $(s\text{-Si})_4/(\text{Ge})_4$ superlattice. To our knowledge, these are the most complete calculations done on any superlattice; the results support the conclusions reached by shifting the LDA eigenvalues, as done here and in Refs. 21 and 22. Brey and Tejedor[20] use the empirical tight binding method to find the superlattice states; however, they did not consider the indirect transitions which we and others[19,21,22] have found to be lower in energy. Wong *et al.*[23] have proposed that the energies are shifted because the layers are not pseudomorphically strained. This issue is not resolvable by present theoretical work and depends upon experimental studies of the actual strain conditions.

ACKNOWLEDGMENTS

We thank C. Mailhiot, T. P. Pearsall, and F. H. Pollak for useful discussions. The present work was supported in part by the U.S. Office of Naval Research through Contract No. N00014-82-C-0244.

*Present address: Department of Physics, University of Missouri–Columbia, Columbia, MO 65211.

†Present address: Department of Physics, University of Illinois at Urbana-Champaign, Urbana, IL 61801.

‡Present address: Phillips Laboratories, 345 Scarborough Road, Briarcliff Manor, NY 10510.

[1]G. C. Osbourn, J. Appl. Phys. **53**, 1586 (1982); T. P. Pearsall, F. H. Pollak, J. C. Bean, and R. Hull, Phys. Rev. B **33**, 6821 (1986).

[2]J. C. Bean, Science **230**, 127 (1985).

[3]T. P. Pearsall, J. Berk, L. C. Feldman, J. M. Bonar, J. P. Mannaerts, and A. Ourmazd, Phys. Rev. Lett. **58**, 729 (1987).

[4]P. Hohenberg and W. Kohn, Phys. Rev. **136**, B864 (1964); W. Kohn and L. J. Sham, *ibid.* **140**, A1133 (1965).

[5]Exchange-correlation potentials are obtained from the calculations of D. M. Ceperley and B. J. Alder, Phys. Rev. Lett. **45**, 566 (1980) as parametrized by J. Perdew and A. Zunger, Phys. Rev. B **23**, 5048 (1981).

[6]G. B. Bachelet, D. R. Hamann, and M. Schluter, Phys. Rev. B **26**, 4199 (1982).

[7]O. H. Nielsen and R. M. Martin, Phys. Rev. B **32**, 3792 (1985).

[8]C. G. Van de Walle and R. M. Martin, Phys. Rev. B **34**, 5621 (1986); see also C. G. Van de Walle, Ph.D. thesis, Stanford University, 1986.

[9]L. J. Sham and M. Schluter, Phys. Rev. Lett. **51**, 1888 (1983).

[10]G. B. Bachelet and N. E. Christensen, Phys. Rev. B **31**, 879 (1985).

[11]F. H. Pollak and M. Cardona, Phys. Rev. **172**, 816 (1968).

[12]M. Chandrasekhar and F. H. Pollak, Phys. Rev. B **15**, 2127 (1977).

[13]L. D. Laude, F. H. Pollak, and M. Cardona, Phys. Rev. B **3**, 2623 (1971).

[14]R. People, J. C. Bean, D. V. Lang, A. M. Sergent, H. L. Störmer, K. W. Wecht, R. T. Lynch, and K. Baldwin, Appl. Phys. Lett. **45**, 1231 (1984); R. People, J. C. Bean, and D. V. Lang, J. Vac. Sci. Technol. A **3**, 846 (1985).

[15]G. Abstreiter, H. Brugger, T. Wolf, H. Jorke, and H. J. Herzog, Phys. Rev. Lett. **54**, 2441 (1985).

[16]L. P. Bouckaert, R. Smolukowski, and E. Wigner, Phys. Rev. **50**, 58 (1936); R. J. Elliott, *ibid.* **96**, 280 (1954).

[17]K. L. Shaklee and R. E. Nahory, Phys. Rev. Lett. **24**, 942 (1970); A. Frova, G. A. Thomas, R. E. Miller, and E. O. Kane, Phys. Rev. Lett. **34**, 1572 (1975); N. O. Lipari and M. Altarelli, Solid State Commun. **18**, 951 (1976).

[18]I. Morrison, M. Jaros, and K. B. Wong, Phys. Rev. B **35**, 9693 (1987).

[19]R. People and S. A. Jackson, Phys. Rev. B **36**, 1310 (1987).

[20]L. Brey and C. Tejedor, Phys. Rev. Lett. **59**, 1022 (1987).

[21]S. Froyen, D. M. Wood, and A. Zunger, Phys. Rev. B **36**, 4547 (1987); **37**, 6893 (1988).

[22]M. S. Hybertsen and M. Schluter, Phys. Rev. B **36**, 9683 (1987).

[23]K. B. Wong, M. Jaros, I. Morrison, and J. P. Hagon, Phys. Rev. Lett. **60**, 2221 (1988).